



## Spike-TBR: a Noise Resilient Neuromorphic Event Representation

Gabriele Magrini<sup>a</sup>, Federico Becattini<sup>b, \*\*</sup>, Luca Cultrera<sup>a</sup>, Lorenzo Berlincioni<sup>a</sup>, Pietro Pala<sup>a</sup>, Alberto Del Bimbo<sup>a</sup>

<sup>a</sup>University of Florence

<sup>b</sup>University of Siena

arXiv:2506.04817v2 [cs.CV] 12 Jun 2025

### ABSTRACT

Event cameras offer significant advantages over traditional frame-based sensors, including higher temporal resolution, lower latency and dynamic range. However, efficiently converting event streams into formats compatible with standard computer vision pipelines remains a challenging problem, particularly in the presence of noise. In this paper, we propose Spike-TBR, a novel event-based encoding strategy based on Temporal Binary Representation (TBR), addressing its vulnerability to noise by integrating spiking neurons. Spike-TBR combines the frame-based advantages of TBR with the noise-filtering capabilities of spiking neural networks, creating a more robust representation of event streams. We evaluate four variants of Spike-TBR, each using different spiking neurons, across multiple datasets, demonstrating superior performance in noise-affected scenarios while improving the results on clean data. Our method bridges the gap between spike-based and frame-based processing, offering a simple noise-resilient solution for event-driven vision applications.

© 2025 Elsevier Ltd. All rights reserved.

### 1. Introduction

Traditional RGB cameras are capable of acquiring the content of a scene and output a stream of RGB frames, typically at rates of about 30 frames per second. When some fast-moving object is present in the scene or when the same camera is rapidly moving with respect to the scene, such a limited frame rate may yield a degradation of the sensing quality with motion blur artifacts in the acquired frames. Another typical limitation of traditional cameras relates to their dynamic range, i.e. the ratio between levels of the brightest and darkest parts of an image: the joint presence of very bright and dark regions can compromise the quality of the acquired scene content in some areas. These limitations are addressed by event cameras, also referred to as neuromorphic cameras, through the use of a different image-acquiring paradigm that produces asynchronous events per pixel whenever an illumination change is detected.

Frame-based cameras capture entire images at regular time intervals, while event cameras only output information when there is a change in the visual scene. This asynchronous nature of event cameras requires adapting vision algorithms to handle these asynchronous data streams. The simplest approach is to accumulate events over time to generate a frame-like representation. Several works use this method [1, 2, 3, 4], which is useful when working with higher-level vision algorithms that expect frames as input. The result of temporal integration can be thought of as an "event-based video", which maintains the advantages of an event camera (e.g., high dynamic range, low power consumption) while presenting the data in a format more amenable to traditional computer vision processing pipelines.

Accumulating events into frame-based representations though has its shortcomings. The accumulation time  $\Delta T$  controlling the time period within which events are gathered controls the trade-off between the temporal granularity at which the data is analyzed and the number of frames that need to be processed. If, on the one hand, small accumulation times allow computer vision pipelines to better exploit the advantages of neuromorphic sensors by capturing fine-grained movements, on the other hand, the amount of information to be processed might make real-time processing unfeasible. Conversely, a large  $\Delta T$  allows fast computation times, but can lead to information loss, as aggregating events often requires some form of quantization.

\*\*Corresponding author

e-mail: [gabriele.magrini@unifi.it](mailto:gabriele.magrini@unifi.it) (Gabriele Magrini),  
[federico.becattini@unisi.it](mailto:federico.becattini@unisi.it) (Federico Becattini),  
[luca.cultrera@unifi.it](mailto:luca.cultrera@unifi.it) (Luca Cultrera),  
[lorenzo.berlincioni@unifi.it](mailto:lorenzo.berlincioni@unifi.it) (Lorenzo Berlincioni),  
[pietro.pala@unifi.it](mailto:pietro.pala@unifi.it) (Pietro Pala), [alberto.delbimbo@unifi.it](mailto:alberto.delbimbo@unifi.it) (Alberto Del Bimbo)

A notable approach that attempts to overcome this trade-off is Temporal Binary Representation (TBR) [5], where each pixel is created by interpreting its event history as a binary string (event/no event) and converting it to a single base-10 value. Despite its simplicity and effectiveness, TBR suffers from a high sensitivity to noise: the presence of noise in recent time slices can yield a flip in the most significant bit, largely changing the resulting representation. An orthogonal strategy for processing event data involves the use of Spiking Neural Networks (SNNs) [6, 7, 8], a type of artificial neural network inspired by the biological functioning of neurons in the brain. In an SNN, neurons communicate with each other via *spikes* or action potentials instead of continuous signals like in traditional artificial neural networks. This theoretically makes SNNs particularly well-suited for processing event data as spikes can directly represent the events generated by an event camera, yet they do not scale well with typical synchronous hardware.

Inspired by the promising properties of SNNs, we propose an enhanced version of TBR that follows a hybrid approach between the spike-based and frame-based paradigms. Our novel encoding strategy, *Spike-TBR*, leverages an SNN layer to accumulate events on its membrane potential (i.e. its current charging state), and we interpret the spikes it fires as the binary digits that make up the TBR representation. The resulting representation is frame-based as TBR, yet it exhibits a highly increased robustness to noise due to the SNN layer, which filters noise by accumulating events into a decaying membrane and fires spikes only when the pixel-wise potential exceeds a threshold. We demonstrate resilience to noise even when training on clean data.

The main contributions are the following: i) we propose Spike-TBR, a noise-resistant frame-based event encoding strategy that overcomes the limitations of TBR [5]; ii) we analyze four different variants of our approach, studying different SNN neurons; iii) we test on four different datasets, obtaining higher or comparable results to state-of-the-art approaches.

## 2. Related Work

Several works have addressed the issue of processing event camera data streams [9]. The interest to adopt traditional computer vision techniques has led to the development of a plethora of strategies to generate event representations, also in the form of event frames [10, 4, 2, 1, 3, 11, 5]. However, most of these approaches commonly apply a temporal quantization in the form of histograms [3] or event subsampling [12]. An alternative approach to processing events is to feed them to specifically tailored architectures, such as Spiking Neural Networks (SNNs). Inspired by the fundamental mechanism of brain computation, SNNs pose themselves as the third generation of neural networks [13], as opposed to the McCulloch-Pitts neuron [14] (first generation) and feedforward and recurrent networks (second generation). The purpose of SNNs is to emulate and reach the computational efficiency of the human brain. Although still far from complete maturity, research on SNNs has seen increasing interest in recent years, driven by the growing need for low-power-consuming neural networks. Thus, they have found applications in various empirical fields, especially

when paired with event-based cameras [6, 7, 8]. To this end, various forms of integration between SNNs and neuromorphic cameras have been proposed and implemented; in [15], the authors present a sensor fusion framework for optical flow estimation, using both frame and event-based sensors data, leveraging the energy-efficiency of SNNs. In [16], a method is proposed for processing data from event cameras using spiking convolutional neural networks (SCNNs), using their sparse and asynchronous nature for efficient visual information processing. [17] proposes a self-supervised framework for estimating optical flow from event camera data using spiking neural networks, all in an end-to-end pipeline between event data and SNN.

Recently, an alternative has also been investigated to take advantage of both the intrinsic temporal richness of SNNs and the computational power of Artificial Neural Networks (ANN), with growing attention for Hybrid Spiking-Artificial Networks [18, 7, 19], developed by implementing SNN layers as temporal encoders that feed features to an ANN decoder to estimate optical flow [7, 19]. Other approaches exploit SNNs to guide attention-based mechanisms taking into account pixel locations of spike activations [18]. Frame-based approaches inspired by SNNs have also been developed, such as the Leaky Surface [20], where a frame-like surface is exploited to keep track of past events: when an event occurs, the pixel at the correspondent coordinate is incremented, while the others decay through time. This concept has also been exploited and adapted in recent works [11]. In this paper, the authors leverage SNN layers to ingest events asynchronously, while synchronously gathering the spikes generated for each pixel and forming a Temporal Binary Representation (TBR) [5]. This offers considerable advantages compared to the original TBR formulation, which is highly noise-sensitive. In fact, SNNs have been proven to have important signal processing properties. The Leaky Integrate and Fire (LIF) [21] declination of SNN has been shown to provide improved robustness and better generalization thanks to its high-frequency signal filtering, thus acting resistant against noisy spikes [22, 23].

## 3. Event Representation

We define the output of an event camera with sensor size  $W \times H$  as a stream of events  $x, y, t, p$ , where  $x \in [1, \dots, H]$  and  $y \in [1, \dots, W]$  denote the spatial coordinates of an event,  $t$  the timestamp at which it occurs, and  $p \in \{-1, +1\}$  its polarity, i.e., the sign of the illumination change. We propose Spike-TBR, an aggregation strategy that groups events occurring within a pre-defined accumulation time  $\Delta T$  into a single frame-based representation. Our solution aims to improve the Temporal Binary Representation (TBR) [5], by reformulating it using spiking layers. In the following we first provide a description of TBR, we provide the details of our proposed representation and we design a classification model exploiting Spike-TBR.

### 3.1. Temporal Binary Representation

The recent Temporal Binary Representation [5] builds frame-based encodings by splitting the accumulation time  $\Delta T$  into  $N$  slices of equal extent  $\Delta t$ . For each slice  $i$ , a binary frame  $b^i$

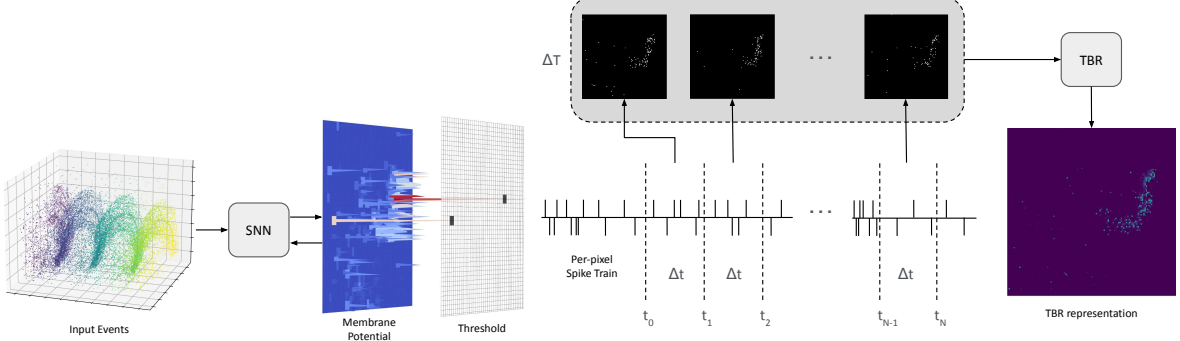


Fig. 1: Spike-TBR pipeline. As the raw event stream is generated by the sensor (left) the SNN membrane accumulates potential  $V(t)$ . Once this potential reaches the threshold  $V_{thr}$  a spike is released. This stream is constantly sampled with a  $\Delta t$  period into binary frames, which every  $\Delta T$  are aggregated into a TBR frame.

is created by checking for the presence or absence of events within the timespan  $[t^i; t^i + \Delta t]$ . It must be noted that, in this formulation, the polarity of events is discarded and only the spatial coordinates are considered. In addition, a single event is sufficient to activate a pixel, thus if more than one event occurs within the same temporal slice, such information is ignored. Formally, each pixel of the binary frame  $b^i$  is defined as  $b_{x,y}^i = \mathbb{1}(x,y)$  where  $\mathbb{1}(x,y)$  is the indicator function returning 1 if at least an event occurred in position  $(x,y)$  and 0 otherwise. The  $N$  consecutive temporal slices are then stacked together into a tensor  $B \in \mathbb{R}^{H \times W \times N}$ . Each spatial coordinate of the tensor can be interpreted as a channel-wise binary string with  $N$  digits  $B_{x,y} = [b_{x,y}^0 \ b_{x,y}^1 \ \dots \ b_{x,y}^{N-1}]$ , where the most significant digit  $b_{x,y}^{N-1}$  indicates the presence of an event in the most recent temporal slice. The final TBR representation is obtained by applying a binary-to-decimal conversion for each pixel, and normalizing the result to fit the  $[0, 1]$  range, by dividing it by  $2^N - 1$ . Such representation condenses into a  $H \times W$  tensor all the information that happened in the accumulation time  $\Delta T$ , losslessly up to a precision of  $\Delta t$ .

### 3.2. Spike-TBR

The downside of the original TBR formulation is its high sensitivity to noise. This stems from the fact that each pixel's representation is derived by viewing its event history as a binary string (event/no event) and then converting this to a single base-10 value. Thus, noise in recent time slices leads to alterations in the most significant bits, resulting in drastically different base-10 representations. In the context of SNNs, the *membrane potential* of a spiking neuron is a time-dependent variable that represents the neuron's internal state,  $V(t)$  that accumulates incoming signals over time and determines whether the neuron emits a spike. To create a representation that is more robust to noise, we combine TBR with a Spiking Neural Network (SNN). SNNs are capable of accumulating asynchronous inputs and producing impulses (spikes), according to the membrane potential that controls the behavior of the neurons: whenever the membrane potential at a given pixel exceeds an internal threshold (which can be either fixed or learnable), a spike spatially located at such pixel is fired. First, we process events with a SNN layer, that accumulates events into its membrane. This module then periodically "reads" the membrane potential

for spike signals, accumulating spikes that occurred in a period of length  $\Delta t$ , rather than accumulating raw events. The benefits of this approach are twofold: on the one hand, isolated events generated by sensor noise are filtered out, on the other hand, depending on the structure of the SNN layer, we can inject learnable parameters directly into the event encoding strategy.

As shown in Fig. 1, by periodically sampling the spike activity of the membrane potential, we can convert the per-pixel spike trains into binary pixel activations. We perform this operation for  $N$  consecutive time slices and we stack the resulting binary frames. Finally, similarly to TBR, we convert the tensor to a base-10 representation and normalize the result. The obtained Spike-TBR representation sacrifices the lossless property of TBR (up to each time slice  $\Delta t$ ), yet makes it much more robust to noise and preserves its compactness as a single frame can summarize spatio-temporal information from the last  $\Delta T = N\Delta t$  temporal interval. In Algorithm 2 we summarize the procedure to generate Spike-TBR representations. We investigate multiple spiking layers, based on neurons with different temporal-dynamics. In the following, we provide an overview of the different kinds of SNN layers that we experimented.

**Leaky Integrate and Fire (LIF)** The first, base approach using SNN for a more robust TBR encoding consists of a single layer using Leaky Integrate and Fire (LIF) neurons [24]. LIF neurons can be modeled as an RC circuit in which the output discharge signal is released after a voltage threshold is reached. It can also be viewed as a system to mimic the behavior of biological neurons by integrating incoming signals over time while also leaking charge. In particular, the differential equation governing the evolution of the membrane potential is given by:

$$\tau_m \frac{dV(t)}{dt} = -(V(t) - V_{rest}) + X(t) \quad (1)$$

where  $\tau_m$  is the membrane time constant,  $V(t)$  the membrane potential at time  $t$ ,  $V_{rest}$  the membrane resting potential, and  $X(t)$  is the input to neuron at time  $t$ . When the membrane potential  $V(t)$  exceeds a threshold  $V_{thr}$ , a spike is emitted and the membrane potential is scaled back to  $V_{rest}$ , such that:

$$S[t] = \begin{cases} 1 & \text{if } V[t] \geq V_{th} \\ 0 & \text{otherwise} \end{cases} \quad (2)$$

where  $S[t]$  is a function that denotes the presence of a spike at

**Algorithm 2** Algorithm for Spike-TBR. Events are accumulated on the membrane potential of a spiking neuron, which generates a spike train for each pixel. Spikes are then accumulated into a single frame interpreting them as a binary string.

```

Require: Event Stream  $E = \{(x_i, y_i, t_i, p_i)\}$ , Time Window  $\Delta T$ , Time
Slice  $\Delta t$ 
Ensure: Encoded Frame  $F$ 
1: Initialize number of TBR bits  $N = \text{int}(\Delta T / \Delta t)$ 
2: Initialize Membrane Potential  $V(x, y) = 0$  for all pixels
3: Initialize Spike Train  $S(x, y, t) = 0$  for all the  $N$  time slices
4: Set Threshold  $V_{\text{thr}}$ 
5: for each event  $(x_i, y_i, t_i, p_i) \in E$  do
6:   Update potential:  $V(x_i, y_i) \leftarrow V(x_i, y_i) + w(p_i)$ 
7:   if  $V(x_i, y_i) \geq V_{\text{thr}}$  then
8:     Generate spike:  $S(x_i, y_i, t_i) = 1$ 
9:     Reset membrane potential:  $V(x_i, y_i) \leftarrow V_{\text{rest}}$ 
10:    end if
11: end for
12: for each pixel  $(x, y)$  do
13:   Convert spike train to binary sequence:

$$B(x, y) = [S(x, y, t_1), S(x, y, t_2), \dots, S(x, y, t_N)]$$

14:   Convert binary sequence to decimal value:

$$F(x, y) = \frac{\sum_{i=0}^{N-1} 2^i \cdot S(x, y, t_i)}{2^N - 1}$$

15: end for
16: return Encoded Frame  $F$ 

```

time  $t$ , and

$$\text{if } V[t] \geq V_{\text{th}}, \quad V[t+1] \rightarrow V_{\text{rest}} \quad (3)$$

Finally, since we are operating at discrete time-steps, we can describe its subthreshold neural dynamics as follows:

$$V[t] = V[t-1] - \frac{1}{\tau_m} (V[t-1] - V_{\text{rest}}) + X[t] \quad (4)$$

Note that this slightly differs from the dynamics described in Eq. 1 as we do not decay the input. On the contrary, we raise the activation threshold to  $V_{\text{th}} = 1.1$  to make the neuron fire only when some information has been accumulated. From Eq. 1, assuming  $V_{\text{rest}} = 0$  and no input  $X[t]$ , we can derive the decay rate of the neuron as

$$\beta = \frac{V[t]}{V[t-1]} = 1 - \frac{1}{\tau_m} \quad (5)$$

which controls the amount of information that gets discarded at each timestep. In this model a single layer of independent LIF neurons sits between the raw data and the TBR encoding. In this way, each pixel is connected to a single LIF neuron, which acts as a filter for noisy spikes, as also hinted in [21]. In particular, in this case the input is left without decay, while the threshold has been slightly increased so that only spikes received in a sufficiently small temporal interval are propagated along the network.

**Recurrent Synapse (RecLIF)** [25] Similarly to the LIF approach, the layer is a 1-on-1 receptive field of LIF neurons.

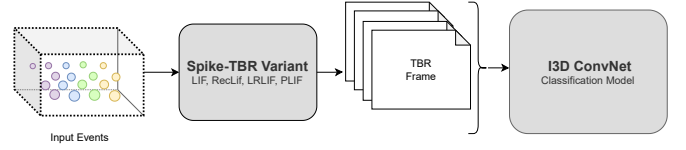


Fig. 2: Pipeline experiment setup. Events are aggregated with Spike-TBR, generating a sequence of TBR frames. Then, a classifier as I3D is used.

In this case, the output of each neuron is propagated back to itself, increasing the effect of spikes and further propagating them through time. This means that for an input  $X[t]$ , the neuron cell will get as actual input:

$$i[t+1] = X[t] + y[t-1] \quad (6)$$

where  $y[t-1]$  is the neuron cell output at time step  $t-1$ .

**Light Refract Synapse (LRLIF)** This approach presents a slight variation of the LIF model [24], in which the reset mechanism changes from total voltage reset to partial inhibition (where after the output spike the internal neuron voltage is reset to 0), with only the spike threshold value subtracted after the spike is emitted from the voltage accumulated in the internal neuron, thus preserving more temporal information. Therefore, we change the reset mechanism from:

$$\text{if } V[t] \geq V_{\text{th}}, \quad V[t+1] \rightarrow V_{\text{rest}} \quad (7)$$

to a softer condition of:

$$\text{if } V[t] \geq V_{\text{th}}, \quad V[t+1] \rightarrow V[t] - V_{\text{th}} \quad (8)$$

**Parametric LIF (PLIF)** Based on the original LIF neuron, the Parametric LIF [26] models the Membrane Time Constant as a learnable parameter to be optimized during training rather than a hyperparameter.

**Classification Model.** As a classification model, we leverage an I3D ConvNet [27] on top of our Spike-TBR frames. Compared to [27], our I3D model follows a different structure. We use a single branch Inception model with Inflated 3D convolutions. Here, the whole sequence of event frames is stacked together as a 3D tensor and processed to obtain a final 256-dimensional feature. It must be noted that through our experiments we do not aim to achieve state-of-the-art performance on benchmarks, but rather to evaluate the effectiveness and robustness of the representation itself compared to the well-established TBR approach [5]. In principle, any other network, specifically tailored for the task at hand, could improve the proposed results. The choice of using an I3D architecture was driven by its success in several event-based tasks in prior works [5, 28, 29, 30]. Our primary focus, however, is evaluating the quality and robustness of the Spike-TBR, especially under noisy conditions. The overall pipeline is shown in Fig.2.

## 4. Experiments

We test our approach on 4 event classification datasets. The *DVSGesture-128* [50] is composed of 1342 hand gestures, with

Table 1: DVSGesture-128 Results.

| Model                       | Acc          |
|-----------------------------|--------------|
| OTT [31]                    | 96.88        |
| DECOLLE [32]                | 97.50        |
| Event-SSM [33]              | 97.70        |
| EGRU [34]                   | 97.80        |
| ST-SNN [35]                 | 98.00        |
| TRIP [36]                   | 98.60        |
| ACE-BET [37]                | 98.88        |
| <b>TBR [5]</b>              | <b>99.62</b> |
| Spike-TBR <sub>LIF</sub>    | <b>99.62</b> |
| Spike-TBR <sub>RecLIF</sub> | <b>99.62</b> |
| Spike-TBR <sub>LRLIF</sub>  | 99.24        |
| Spike-TBR <sub>PLIF</sub>   | <b>99.62</b> |

Table 2: DVSLip Results.

| Model                       | Acc          |
|-----------------------------|--------------|
| S-MSTP [38]                 | 60.20        |
| Rn-net [39]                 | 67.50        |
| Action-net [40]             | 68.80        |
| G2N2 [41]                   | 69.40        |
| MSTP [38]                   | 72.10        |
| MTGA [42]                   | 75.08        |
| SpikGRU2+ [43]              | 75.30        |
| <b>TBR [5]</b>              | 70.00        |
| Spike-TBR <sub>LIF</sub>    | <b>75.91</b> |
| Spike-TBR <sub>RecLIF</sub> | 74.45        |
| Spike-TBR <sub>LRLIF</sub>  | 71.53        |
| Spike-TBR <sub>PLIF</sub>   | 74.45        |

Table 3: NCaltech-101 Results.

| Model                       | Acc          |
|-----------------------------|--------------|
| TEBN [44]                   | 63.13        |
| BackEISNN [45]              | 65.53        |
| ST-SNN [35]                 | 71.20        |
| Spikformer [46]             | 72.83        |
| SSNN [47]                   | 77.97        |
| NDA-SNN [48]                | 78.20        |
| Eventmix [49]               | <b>79.47</b> |
| <b>TBR [5]</b>              | 72.50        |
| Spike-TBR <sub>LIF</sub>    | 68.30        |
| Spike-TBR <sub>RecLIF</sub> | 69.17        |
| Spike-TBR <sub>LRLIF</sub>  | 68.08        |
| Spike-TBR <sub>PLIF</sub>   | 69.28        |

Table 4: MICCGesture results.

| Model                       | Acc          |
|-----------------------------|--------------|
| Polarity [5]                | 68.40        |
| SAE [5]                     | 70.13        |
| <b>TBR [5]</b>              | <b>73.16</b> |
| Spike-TBR <sub>LIF</sub>    | <b>73.16</b> |
| Spike-TBR <sub>RecLIF</sub> | 66.66        |
| Spike-TBR <sub>LRLIF</sub>  | 64.06        |
| Spike-TBR <sub>PLIF</sub>   | 66.23        |

an average duration of 6 seconds. Samples are split into 11 classes, 10 gestures plus a distractor. The recordings comprise 29 subjects under different illumination conditions, and were made using a DVS128 camera ( $128 \times 128$ px resolution). The *MICCGesture* dataset [5] was recorded by 7 different actors of different age, height and gender for a total of 231 videos. It was designed as an extension of DVSGesture-128, and comprises the same gestures at different speeds. It was recorded using a higher resolution of  $640 \times 480$ . The *DVSLip* dataset [51] is a collection of event-based lip-reading videos recorded with a DAVIS346 camera ( $346 \times 260$ px resolution) from 40 subjects reading sequences of words. Finally, the *NCaltech-101* dataset [52] is a neuromorphic conversion of Caltech101 [53] obtained by recording the original data with an event camera. It is a classification task with 100 classes. The results are shown in two sets of experiments: comparison with state-of-the-art models and robustness of the model under noisy conditions. For all the experiments we use 8 bits for TBR and, depending on the dataset, we use slightly different settings for the accumulation time. We use a  $\Delta t = 2.5ms$  for DVSGesture-128, NCalTech-101 and MICCGesture, while  $\Delta t = 6.25ms$  for DVSLip, as events streams are sparser. The choice of  $\Delta t$  is based on the characteristics of each dataset. For datasets with denser event streams (DVSGesture-128, MICCGesture, NCaltech-101), we use a smaller accumulation time to retain finer temporal details, which might otherwise be lost. Conversely, for DVSLip, which has sparser event streams, we increase the accumulation time to prevent excessive sparsity in the encoded frames. Sparsity is a direct consequence of how subjects move in the recorded scene, as fast movements yield a much higher event rate (thus, a dense stream), whereas slower movements, as found in DVSLip, result in sparser streams as less events are generated. Similarly, we consider non-overlapping chunks of 500ms as separate samples at training time on DVSGesture-128, NCalTech-101 and MICCGesture, yet for DVSLip we use entire sequences instead. At test time we use chunks of the same lengths and perform a majority voting for the final classification. All the Spike Neural Network experiments have been implemented using the *spikingjelly* [54] and the *tonic* [55] libraries.

#### 4.1. State-of-the-art Comparison

In Tabs. 1, 2, 3 and 4 we report the accuracies of our approach compared to state of the art methods. All results are taken from publicly available benchmarks, whereas we run all TBR [5] experiments with our pipeline to establish a fair comparison. For all the LIF variants, except PLIF which has learnable parameters, we tune the decay rate *beta* on a held-out validation set. We use  $\beta = 0.5, 0.9, 0.7, 0.7$ , respectively for DVSGesture-128, DVSLip, NCaltech-101 and MICCGesture.

On DVSGesture-128 (Tab. 1), we achieve an accuracy of 99.62% with most models, on par with the vanilla TBR representation [5]. It must be said that the DVSGesture-128 dataset is simple and saturated, however, the results confirm that Spike-TBR is capable of matching or improving upon other state-of-the-art approaches. Tab. 2 reports the results on DVSLip [51]. Interestingly, all variants of Spike-TBR yield improved results compared to TBR. In particular, the LIF neuron is able to obtain state-of-the-art results, followed closely by PLIF and surpassing previous best-performing methods such as MTGA [42] and SpikGRU2+ [43]. The results highlight that our proposed models maintain strong accuracy even in tasks requiring fine-grained motion understanding, such as lip movements. Tab. 3 shows the classification accuracy on NCaltech-101 [52] dataset. On this benchmark, Eventmix [49] and NDA-SNN [48] models, which leverage intensive data augmentation strategies, show the highest accuracies, ranking higher than all Spike-TBR variants. However, we obtain slightly lower results compared to vanilla TBR, showing that the spiking layers can be introduced in the encoding strategy without severe side effects. It must be noted that NCaltech-101 is the only dataset where we report lower results than TBR. We attribute this to the fact that the dataset is collected by recording a screen and events appear in bursts corresponding to the saccadic movements performed to make the signal visible to the camera. This unnatural stream of events makes it hard for spiking neural networks to accumulate information in the membrane correctly. Finally, in Tab. 4 we report a comparison with state-of-the-art methods on the MICCGesture dataset. Spike-TBR<sub>LIF</sub> matches the accuracy of TBR, confirming the quality of the event encoding strategy. The experiments on the four datasets show that Spike-TBR consistently provides comparable or superior results to TBR, setting a strong founda-



Fig. 3: Impact of noise on binary event frames and filtering properties of Spiking Neurons. **Top:** consecutive frames extracted directly from the four datasets used in this paper. **Center:** the impact of 1% noise on the same frames. **Bottom:** the output of the LIF receptive field using the noisy images as input.

tion for our subsequent analysis in noise-affected environments. In general, these improvements are primarily due to the combination of frame-based and event-based encodings and to the noise-resistant properties introduced by spiking neurons. Additionally, the usage of learnable parameters (PLIF variant) can further optimize event aggregation.

#### 4.2. Sensitivity to Noise

To assess the robustness to noise of Spike-TBR compared to TBR [5], we inject noise into the event streams. To simulate a given amount of noise  $p$  (say  $p = 0.01$  for 1%), we add an event every  $\Delta t$  ms with probability  $p$  for each pixel. Therefore, each TBR slice has, on average,  $p \times H \times W$  noise events, where  $H$  and  $W$  are the height and width of the frame. Since a TBR frame is composed of  $N$  slices, noise injection can alter up to  $p \times H \times W \times N$  pixels in the final representation. This setup allows us to analyze the resilience of our spiking-based models, which are designed to filter out noise and fire only if the membrane reaches sufficient potential, as shown in Fig. 3, where binary frames generated by Spike-TBR<sub>LIF</sub> are shown.

Fig. 4 shows the impact of increasing noise levels on classification accuracy. Across all datasets, Spike-TBR significantly enhances the robustness to noise compared to vanilla TBR. On DVSGesture-128 (Fig. 4a) the accuracy of TBR declines rapidly as noise increases, whereas all variations of Spike-TBR maintain a higher accuracy even for large quantities of noise. Similar trends are observed on MICCGesture (Fig. 4b), although overall accuracies are lower due to the higher complexity of the dataset and all models do not tolerate well large amounts of noise. For DVSLip (Fig. 4c), which involves more subtle lip movements, the gap between TBR and Spike-TBR is still evident, although there is a more appreciable difference between different spike neurons. In particular, the PLIF neuron, which has learnable parameters, outperforms all other variants. Finally, the NCALTECH-101 dataset (Fig. 4d) poses a more challenging task due the presence of saccadic movements that make

Table 5: Effect of training TBR with noise injection at training time. The model proves to be more robust to the specific amount of noise, but it quickly degrades when more noise is added. Spike-TBR instead demonstrates to be more robust.

| Noise                    | 0.0          | 0.001        | 0.01         | 0.02         | 0.05        |
|--------------------------|--------------|--------------|--------------|--------------|-------------|
| TBR                      | <b>99.62</b> | 80.30        | 40.50        | 9.46         | <b>9.09</b> |
| TBR + noise aug. (0.001) | <b>99.62</b> | <b>99.62</b> | 11.74        | 9.09         | <b>9.09</b> |
| TBR + noise aug. (0.01)  | 98.86        | 98.48        | <b>99.24</b> | 9.46         | <b>9.09</b> |
| Spike-TBR <sub>LIF</sub> | <b>99.62</b> | <b>99.62</b> | 93.94        | <b>42.80</b> | <b>9.09</b> |

Table 6: We inject in each TBR slice the amount of noise taken from a Prophe-see EVK4 equal to 2.5ms, 5ms, 25ms and 50ms. Spike-TBR, although trained on synthetic random noise, still exhibits higher robustness.

| Real Noise               | 2.5ms        | 5ms          | 25ms         | 50ms         |
|--------------------------|--------------|--------------|--------------|--------------|
| TBR                      | 98.10        | 20.83        | 9.09         | 9.09         |
| Spike-TBR <sub>LIF</sub> | <b>99.24</b> | <b>97.77</b> | <b>84.47</b> | <b>19.69</b> |

noise filtering harder. However, RecLIF and PLIF show greater robustness, maintaining a consistently higher accuracy across noise levels compared to TBR. In conclusion Fig. 4 shows that, across all datasets, the spike-based approaches (LIF, RecLIF, LRLIF and PLIF) outperform TBR in noisy conditions.

We perform an additional control study, by training TBR non-spiking models with noise injected at training time to establish the effect of a simple data augmentation strategy. The model indeed improves its robustness when the amount of noise used at training time is equivalent to the one added at test time. However, with higher noise, the model quickly degrades. We show in Tab. 5 the results of training TBR with noise 0.001 and 0.01. This behavior occurs since the model overfits such noise levels, failing to generalize to higher ones. Moreover, the model degrades in performance also in the non-noisy scenario depending on the quantity of noise seen in training. Spike-TBR instead offers a robust alternative without prior knowledge of the noise level that will be encountered at test time.

It must be noted that in all our experiments we used synthetic random noise. However, other types of noise (sensor noise, thermal noise, pixel defects, etc.) might be distributed differently. Yet, modeling these sources of noise is not straightforward. To test on realistic noise, we first recorded a static background to gather real noise generated by an event camera<sup>1</sup>. Then, we added the noise to the original event videos, resizing them to match the dataset’s frame size. We show in Tab. 6 results on the DVS-Gesture dataset. For each TBR slice, we inject a number of events equal to a slice of noise of length 2.5ms, 5ms, 25ms and 50ms. Spike-TBR still filters the noise out and performs well, even when trained on synthetic random noise.

#### 4.3. Effect of Decay Rate

In all the variants of the LIF neuron, the  $\beta$  parameter, defined in Eq. 5 plays a decisive role in how noise is handled. In fact, the parameter controls the decay of the membrane potential through time, thus affecting the amount of time the information is retained by the neuron. In Tab.7 we report an ablation study, varying the parameter in Spike-TBR<sub>LIF</sub> on two datasets, namely DVSGesture-128 [50] and DVSLip [51]. In particular, we study the effect of  $\beta$  on different noise levels. Interest-

<sup>1</sup>Prophe-see Evaluation Kit 4 (EVK4), with IMX646 neuromorphic sensor

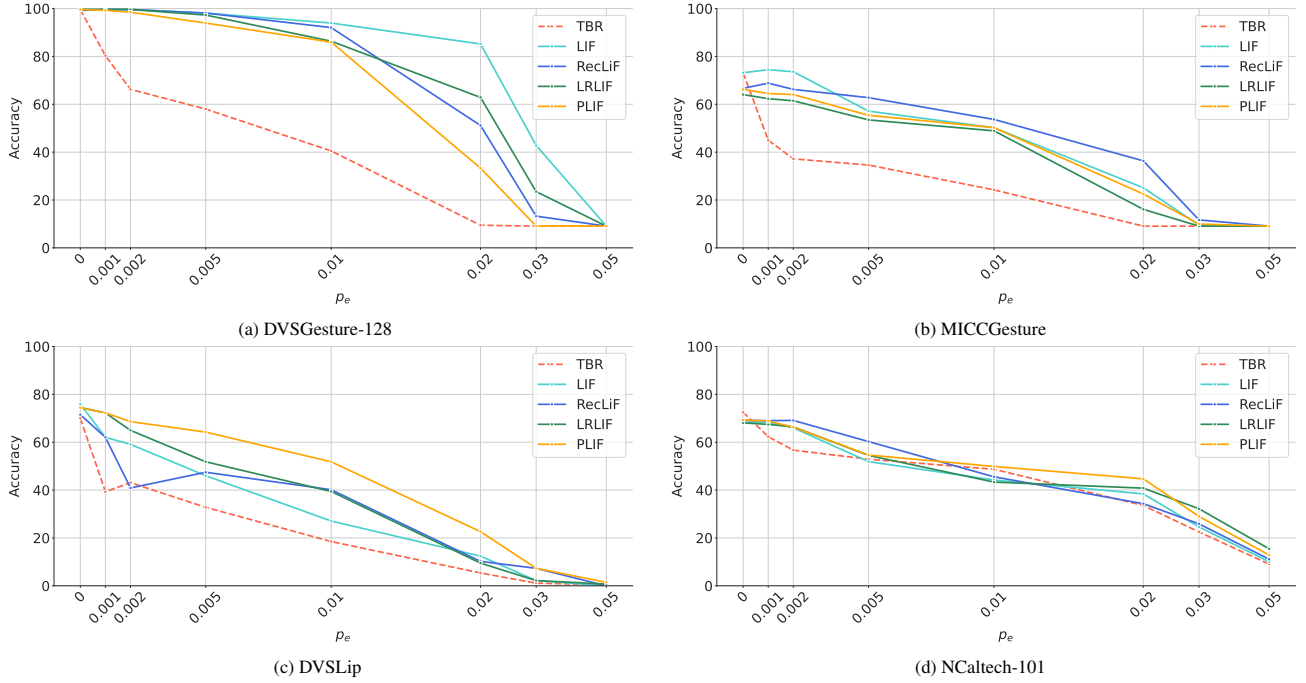


Fig. 4: Noise-affected performances on the tested datasets based on the different spiking neuronal architecture. Plots (a), (b), (c), and (d) correspond to DVSGesture-128, MICCGesture, DVSLip, and NCaltech-101, respectively. In all the instances, the augmented resilience with respect to the accuracy is clearly noticeable in the architectures involving a Spiking Neuron as noise filtering, compared to the catastrophic impact of the noise on the base I3D network.

Table 7: Effect of the parameter  $\beta$  on Spike-TBR<sub>LIF</sub>. Different  $\beta$  yield a considerably different sensitivity to noise.

| Noise         | DVSGesture-128 |              |              |              |              | DVSLip       |              |              |             |             |
|---------------|----------------|--------------|--------------|--------------|--------------|--------------|--------------|--------------|-------------|-------------|
|               | 0.0            | 0.005        | 0.01         | 0.03         | 0.05         | 0.0          | 0.005        | 0.01         | 0.03        | 0.05        |
| $\beta = 0.3$ | 98.10          | 96.96        | <b>95.36</b> | <b>82.90</b> | <b>19.70</b> | 45.99        | 11.68        | 3.65         | 0.73        | <b>0.73</b> |
| $\beta = 0.5$ | <b>99.60</b>   | <b>98.10</b> | 93.94        | 42.80        | 9.09         | 65.69        | 24.09        | 6.57         | 0.73        | 0.00        |
| $\beta = 0.7$ | <b>99.60</b>   | 96.21        | 90.15        | 9.09         | 9.09         | 67.15        | 33.58        | 8.02         | 0.00        | 0.00        |
| $\beta = 0.9$ | <b>99.60</b>   | 91.28        | 79.16        | 9.09         | 9.09         | <b>75.91</b> | <b>45.99</b> | <b>27.07</b> | <b>2.19</b> | 0.00        |

ingly, depending on the dataset, the parameter has an opposite effect: on DVSGesture-128 a small  $\beta$  yields a higher resistance to noise, whereas on DVSLip the same is achieved with a high value of  $\beta$ . The reason for this opposite behavior can be found in the nature of the data. In fact, streams in the DVSLip dataset exhibit a much lower event rate compared to DVSGesture-128, hence relevant information is easily discarded as the membrane decays. On the opposite, DVSGesture-128 videos have a high event rate, which allows the neurons to retain the signal even with small  $\beta$ , discarding the noise effectively.

#### 4.4. Computational Analysis

We compute SNN-related metrics [56]: ACs (accumulated computation per synaptic operation only upon the receipt of an incoming spike) and MACs (multiply-accumulate computations per synaptic operation). The AC operations are those performed by the SNN, the MAC operations are instead performed by the rest of the architecture (I3D). On DVSGesture-128, on average, the model performs 50.18K ACs and 194.11M MACs, thus resulting in a negligible overhead for the SNN (+0.02%).

## 5. Conclusions

We introduced Spike-TBR, a noise-robust event encoding approach that enhances Temporal Binary Representation (TBR) [5] by leveraging the inherent temporal dynamics of spiking neural networks. Our method addresses key limitations of TBR, particularly its sensitivity to noise, by integrating spiking neurons to filter noisy events and preserve critical spatio-temporal information. Experiments across several datasets demonstrate that Spike-TBR achieves competitive performance on clean data, while it significantly outperforms the traditional approach under noisy conditions. The proposed method effectively balances compact event-based representation with enhanced noise robustness, offering a promising avenue for further research in event-driven vision tasks. A limitation of the proposed approach, that is worth exploring in future work, includes the fact that the encoding strategy may require fine-tuning when applied to different neuromorphic cameras. Future work will explore training with noise augmentation, evaluating on real-world applications, and extending Spike-TBR to other event-based tasks such as optical flow and object tracking.

## References

- [1] A. Nguyen, T.-T. Do, D. G. Caldwell, N. G. Tsagarakis, Real-time 6dof pose relocalization for event cameras with stacked spatial lstm networks, in: Proceedings of the IEEE CVPR Workshops, 2019, pp. 0–0.
- [2] S. Miao, G. Chen, X. Ning, Y. Zi, K. Ren, Z. Bing, A. Knoll, Neuromorphic vision datasets for pedestrian detection, action recognition, and fall detection, Frontiers in neurorobotics 13 (2019) 38.
- [3] R. Ghosh, A. Gupta, A. Nakagawa, A. Soares, N. Thakor, Spatiotemporal filtering for event-based action recognition, arXiv preprint arXiv:1903.07067 (2019).

[4] M. Cannici, M. Ciccone, A. Romanoni, M. Matteucci, A differentiable recurrent surface for asynchronous event-based data, in: ECCV, 2020.

[5] S. U. Innocenti, F. Becattini, F. Pernici, A. Del Bimbo, Temporal binary representation for event-based action recognition, in: ICPR, IEEE, 2021, pp. 10426–10432.

[6] Q. Liu, D. Xing, H. Tang, D. Ma, G. Pan, Event-based action recognition using motion information and spiking neural networks., in: IJCAI, 2021.

[7] C. Lee, A. K. Kosta, A. Z. Zhu, K. Chaney, K. Daniilidis, K. Roy, Spike-flownet: event-based optical flow estimation with energy-efficient hybrid neural networks, in: ECCV, 2020, pp. 366–382.

[8] J. Cuadrado, U. Rançon, B. R. Cottereau, F. Barranco, T. Masquelier, Optical flow estimation from event-based cameras and spiking neural networks, *Frontiers in Neuroscience* 17 (2023) 1160034.

[9] G. Gallego, T. Delbrück, G. Orchard, C. Bartolozzi, B. Taba, A. Censi, S. Leutenegger, A. Davison, J. Conradt, K. Daniilidis, et al., Event-based vision: A survey, *arXiv preprint arXiv:1904.08405* (2019).

[10] D. Gehrig, A. Loquercio, K. Derpanis, D. Scaramuzza, End-to-end learning of representations for asynchronous event-based data, in: 2019 IEEE/CVF ICCV, IEEE Computer Society, Los Alamitos, CA, USA, 2019, pp. 5632–5642.

[11] M. Cannici, M. Ciccone, A. Romanoni, M. Matteucci, Asynchronous convolutional networks for object detection in neuromorphic cameras, in: Proceedings of the IEEE CVPR Workshops, 2019, pp. 0–0.

[12] J. Kaiser, A. Friedrich, J. Tieck, D. Reichard, A. Roennau, E. Neftci, R. Dillmann, Embodied neuromorphic vision with event-driven random backpropagation, *arXiv preprint arXiv:1904.04805* (2019).

[13] W. Maass, Networks of spiking neurons: the third generation of neural network models, *Neural networks* 10 (1997) 1659–1671.

[14] W. S. McCulloch, W. Pitts, A logical calculus of the ideas immanent in nervous activity, *bulletin of mathematical biophysics* (1943) 115–133.

[15] C. Lee, A. K. Kosta, K. Roy, Fusion-flownet: Energy-efficient optical flow estimation using sensor fusion and deep fused spiking-analog network architectures, in: 2022 ICRA, IEEE, 2022, pp. 6504–6510.

[16] L. Cordone, B. Miramond, S. Ferrante, Learning from event cameras with sparse spiking convolutional neural networks, in: 2021 IJCNN, IEEE, 2021, pp. 1–8.

[17] J. Hagenaars, F. Paredes-Vallés, G. De Croon, Self-supervised learning of event-based optical flow with spiking neural networks, *NeurIPS* 34 (2021) 7167–7179.

[18] Z. Yang, Y. Wu, G. Wang, Y. Yang, G. Li, L. Deng, J. Zhu, L. Shi, Dashnet: A hybrid artificial and spiking neural network for high-speed object tracking, *arXiv preprint arXiv:1909.12942* (2019).

[19] S. Negi, D. Sharma, A. K. Kosta, K. Roy, Best of both worlds: Hybrid snn-ann architecture for event-based optical flow estimation, *arXiv preprint arXiv:2306.02960* (2023).

[20] G. K. Cohen, Event-based feature detection, recognition and classification, Ph.D. thesis, Western Sydney University (Australia), 2015.

[21] S. S. Chowdhury, C. Lee, K. Roy, Towards understanding the effect of leak in spiking neural networks, *Neurocomputing* 464 (2021) 83–94.

[22] S. Park, D. Lee, S. Yoon, Noise-robust deep spiking neural networks with temporal information, in: 2021 58th ACM/IEEE DAC, IEEE, 2021.

[23] T. K. T. Thieu, R. Melnik, Effects of noise on leaky integrate-and-fire neuron models for neuromorphic computing applications, in: Computational Science and Its Applications, Cham, 2022, pp. 3–18.

[24] W. Maass, C. M. Bishop, Pulsed neural networks, MIT press, 2001.

[25] B. Yin, F. Corradi, S. M. Bohté, Effective and efficient computation with multiple-timescale spiking recurrent neural networks, in: International Conference on Neuromorphic Systems 2020, 2020, pp. 1–8.

[26] W. Fang, Z. Yu, Y. Chen, T. Masquelier, T. Huang, Y. Tian, Incorporating learnable membrane time constant to enhance learning of spiking neural networks, in: Proceedings of the IEEE/CVF ICCV, 2021, pp. 2661–2671.

[27] J. Carreira, A. Zisserman, Quo vadis, action recognition? a new model and the kinetics dataset, in: proceedings of the IEEE CVPR, 2017.

[28] L. Berlincioni, L. Cultrera, C. Albisani, L. Cresti, A. Leonardo, S. Pichichoni, F. Becattini, A. Del Bimbo, Neuromorphic event-based facial expression recognition, in: Proceedings of the IEEE/CVF CVPR, 2023.

[29] L. Berlincioni, L. Cultrera, F. Becattini, A. Del Bimbo, Neuromorphic valence and arousal estimation, *arXiv preprint arXiv:2401.16058* (2024).

[30] F. Becattini, L. Cultrera, L. Berlincioni, C. Ferrari, A. Leonardo, A. Del Bimbo, Neuromorphic facial analysis with cross-modal supervision, *arXiv preprint arXiv:2409.10213* (2024).

[31] M. Xiao, Q. Meng, Z. Zhang, D. He, Z. Lin, Online training through time for spiking neural networks, *NeurIPS* 35 (2022) 20717–20730.

[32] J. Kaiser, H. Mostafa, E. Neftci, Synaptic plasticity dynamics for deep continuous local learning, *Frontiers in Neuroscience* 14 (2020) 424.

[33] M. Schöne, N. M. Sushma, J. Zhuge, C. Mayr, A. Subramoney, D. Kappel, Scalable event-by-event processing of neuromorphic sensory signals with deep state-space models, *arXiv preprint arXiv:2404.18508* (2024).

[34] A. Subramoney, K. K. Nazeer, M. Schöne, C. Mayr, D. Kappel, Efficient recurrent architectures through activity sparsity and sparse back-propagation through time, *arXiv preprint arXiv:2206.06178* (2022).

[35] X. She, S. Dash, S. Mukhopadhyay, Sequence approximation using feed-forward spiking neural network for spatiotemporal learning: Theory and optimization methods, in: ICLR, 2022.

[36] C. Arjmand, Y. Xu, K. Shidqi, A. F. Dobrita, K. Vadivel, P. Detterer, M. Sifalakis, A. Yousefzadeh, G. Tang, Trip: Trainable region-of-interest prediction for hardware-efficient neuromorphic processing on event-based vision, *arXiv preprint arXiv:2406.17483* (2024).

[37] C. Liu, X. Qi, E. Y. Lam, N. Wong, Fast classification and action recognition with event-based imaging, *IEEE access* 10 (2022) 55638–55649.

[38] H. Bulzomi, M. Schweiker, A. Gruel, J. Martinet, End-to-end neuromorphic lip-reading, in: Proceedings of the IEEE/CVF CVPR, 2023.

[39] S. Yoo, E. Y.-J. Lee, Z. Wang, X. Wang, W. D. Lu, Rn-net: Reservoir nodes-enabled neuromorphic vision sensing network, *Advanced Intelligent Systems* (2024) 2400265.

[40] Z. Wang, Q. She, A. Smolic, Action-net: Multipath excitation for action recognition, in: Proceedings of the IEEE/CVF CVPR, 2021.

[41] T. Mesquida, M. Dampfhofer, T. Dalgaty, P. Vivet, A. Sironi, C. Posch, G2n2: Lightweight event stream classification with gru graph neural networks, in: BMVC, 2023, p. 660.

[42] W. Zhang, J. Wang, Y. Luo, L. Yu, W. Yu, Z. He, Mtga: Multi-view temporal granularity aligned aggregation for event-based lip-reading, *arXiv preprint arXiv:2404.11979* (2024).

[43] M. Dampfhofer, T. Mesquida, Neuromorphic lip-reading with signed spiking gated recurrent units, in: Proceedings of the IEEE/CVF CVPR, 2024, pp. 2141–2151.

[44] C. Duan, J. Ding, S. Chen, Z. Yu, T. Huang, Temporal effective batch normalization in spiking neural networks, *NeurIPS* 35 (2022).

[45] D. Zhao, Y. Zeng, Y. Li, Backeisnn: A deep spiking neural network with adaptive self-feedback and balanced excitatory–inhibitory neurons, *Neural Networks* 154 (2022) 68–77.

[46] Z. Zhou, Y. Zhu, C. He, Y. Wang, S. Yan, Y. Tian, L. Yuan, Spikformer: When spiking neural network meets transformer, *arXiv preprint arXiv:2209.15425* (2022).

[47] Y. Ding, L. Zuo, M. Jing, P. He, Y. Xiao, Shrinking your timestep: Towards low-latency neuromorphic object recognition with spiking neural networks, in: Proceedings of AAAI, volume 38, 2024, pp. 11811–11819.

[48] Y. Li, Y. Kim, H. Park, T. Geller, P. Panda, Neuromorphic data augmentation for training spiking neural networks, in: ECCV, 2022, pp. 631–649.

[49] G. Shen, D. Zhao, Y. Zeng, Eventmix: An efficient data augmentation strategy for event-based learning, *Information Sciences* (2023) 119170.

[50] A. Amir, B. Taba, D. Berg, T. Melano, J. McKinstry, C. Di Nolfo, T. Nayak, A. Andreopoulos, G. Garreau, M. Mendoza, et al., A low power, fully event-based gesture recognition system, in: Proceedings of the IEEE CVPR, 2017.

[51] G. Tan, Y. Wang, H. Han, Y. Cao, F. Wu, Z.-J. Zha, Multi-grained spatio-temporal features perceived network for event-based lip-reading, in: Proceedings of the IEEE/CVF CVPR, 2022, pp. 20094–20103.

[52] G. Orchard, A. Jayawant, G. K. Cohen, N. Thakor, Converting static image datasets to spiking neuromorphic datasets using saccades, *Frontiers in Neuroscience* 9 (2015).

[53] L. Fei-Fei, R. Fergus, P. Perona, Learning generative visual models from few training examples: An incremental bayesian approach tested on 101 object categories, in: CVPR Workshop, 2004, pp. 178–178.

[54] W. Fang, Y. Chen, J. Ding, Z. Yu, T. Masquelier, D. Chen, L. Huang, H. Zhou, G. Li, Y. Tian, Spikingjelly: An open-source machine learning infrastructure platform for spike-based intelligence, *Science Advances* 9 (2023) eadi1480.

[55] G. Lenz, K. Chaney, S. B. Shrestha, O. Oubari, S. Picaud, G. Zarrella, Tonic: event-based datasets and transformations., 2021.

[56] G. Chen, P. Peng, G. Li, Y. Tian, Training full spike neural networks via auxiliary accumulation pathway, *arXiv preprint arXiv:2301.11929* (2023).